physica status solidi a
www.pss-a.com
applications and materials science

Parameter extraction from S-shaped current–voltage characteristics in organic photocell with opposed two-diode model: Effects of ideality factors and series resistance

Kazuya Tada*

Division of Electrical Engineering, University of Hyogo, 2167 Shosha, Himeji, Hyogo 671-2280, Japan

* e-mail tada@eng.u-hyogo.ac.jp, Phone: +81-79-267-4966, Fax: +81-79-267-4855

Non-traditional photocells such as organic photocells frequently show S-shaped current–voltage characteristics, which can be reproduced with not the simple one-diode equivalent-circuit model but an opposed two-diode model. In this study, a facile method for the extraction of the device parameters from S-shaped characteristics of a photocell using the opposed two-diode model is demonstrated. It was found that the fitting accuracy is insensitive to the ideality factors of the diodes. Moreover, contrary to the preceding studies, the exclusion of the series resistance was found to have a noticeable impact on the fitting results.

1 Introduction Solution-processed photocells including those using organic materials and inorganic materials have been attracting much attention of researchers, because they are believed to deliver cheap and environmental-friendly energy source required in the next generation [1–3]. Extracting device parameters of a photocell by fitting the current–voltage characteristics with a simple one-diode model shown in Fig. 1a is routinely carried out in order to obtain better understanding of the device performance [4, 5].

On the other hand, in the study on the non-traditional photocells, it is frequently observed that some devices show S-shaped current–voltage curve, which is commonly referred to as a sign of deteriorated composite/metal interfaces [6, 7] and cannot be reproduced with the simple one-diode model. Although its physical meaning has not been fully clarified yet, it has been reported that an opposed two-diode model, in which the second diode with a parallel resistor opposed to the diode in the one-diode model is added as shown in Fig. 1b, can reproduce the S-shaped curve [7, 8]. The extraction of the device parameters of a photocell by fitting the current–voltage characteristics with the simple one-diode model does not seem to be recognized as an easy task, since the development of efficient and stable

calculation techniques for this purpose is still being an active research area [9–11]. Thus, the analysis of the S-shaped current–voltage characteristics with the opposed two-diode model, which requires more efforts in calculation than the one-diode model, is rarely reported.

In this study, a simple and effective method utilizing commercial spreadsheet software to extract the device parameters of photocells showing S-shaped current–voltage characteristics by fitting the characteristics with opposed two-diode model is presented. The experimental data of a solution-processed small molecular bulk heterojunction photocells using a composite consisting of p-DTS(FBTTh$_2$)$_2$ and neat C$_{70}$ [12] are used to test the method proposed.

2 Models and methods The current (I)–voltage (V) characteristics of the one-diode model of photocell shown in Fig. 1a is described by the equation

$$I = I_{s1} \cdot \left(\exp\left(\frac{V - I \cdot R_s}{n_1 \cdot V_t} \right) - 1 \right) + \frac{V - I \cdot R_s}{R_{p1}} - I_{ph}, \quad (1)$$

where R_s, R_{p1}, are the series and parallel (shunt) resistance respectively, and I_{s1} and n_1 are the reverse saturation current
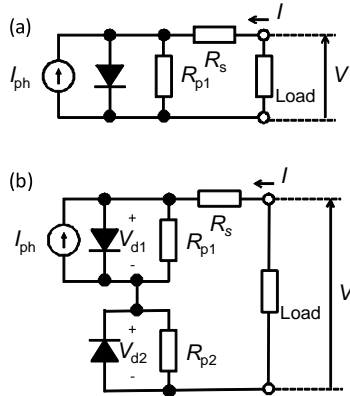
Figure 1 (a) One-diode and (b) opposed two-diode equivalent-circuit models of photocell.

and the ideality factor of the diode, respectively, and I_{ph} is the ideal photocurrent. At room temperature, the thermal voltage V_t is approximately $26\,mV$.

This transcendental equation can be solved for neither I in terms of V nor V in terms of I by using common elementary functions. Therefore, the equation is usually solved by iterative algorithms such as bisection method. This gives a difficulty in the curve fitting process, because the endpoint values for searching interval must be specified for the bisectional method, and choosing inadequate endpoints results in either upsurge of computational efforts or convergence failure. Newton's method, another popular way to solve the equation numerically, has the initial value problem. In this context, it has been reported that the current–voltage characteristics can be explicitly described by using the Lambert W-function, which is defined as the solution of the transcendental equation $W(x)\exp[W(x)]=x$, as follows [13, 14]:

$$
I(V) = \frac{n_1 \cdot V_t}{R_s}
$$

$$
\times W_0\left(\frac{I_{s1} \cdot R_s}{n_1 \cdot V_t \cdot \left(1 + \frac{R_s}{R_{p1}}\right)} \cdot \exp\left(\frac{V + (I_{s1} + I_{ph}) \cdot R_s}{n_1 \cdot V_t \cdot \left(1 + \frac{R_s}{R_{p1}}\right)}\right)\right)
$$

$$
+ \frac{\frac{V}{R_{p1}} - (I_{s1} + I_{ph})}{1 + \frac{R_s}{R_{p1}}} \tag{2}
$$

or

$$
V(I) = -n_1 \cdot V_t \cdot W_0\left(\frac{I_{s1} \cdot R_{p1}}{n_1 \cdot V_t} \cdot \exp\left(\frac{(I + I_{s1} + I_{ph}) \cdot R_{p1}}{n_1 \cdot V_t}\right)\right)
$$

$$
+ I \cdot R_s + R_{p1} + (I_{s1} + I_{ph}) \cdot R_{p1}. \tag{3}
$$

The Lambert W-function has two real branches, and $W_0(x)$ denotes so-called upper branch defined for $x \in [-\exp(-1), +\infty]$. Another branch is defined only for $x < 0$ and we do not need to care about it in the present study.

Although $W_0(x)$ is not as common as the natural logarithmic function or the inverse trigonometric functions such as the arctangent function, compact and rapid computational algorithms for $W_0(x)$ are known [15–17]. This makes these explicit expressions quite useful and thus the irritating factor in the curve fitting process mentioned above can be removed.

For the opposed two-diode model shown in Fig. 1b, the current–voltage equation solved for V in terms of I can be expressed as follows [18]:

$$
V(I) = V_{d1}(I) + V_{d2}(I) + I \cdot R_s, \tag{4}
$$

where

$$
V_{d1}(I) = -n_1 \cdot V_t \cdot W_0\left(\frac{I_{s1} \cdot R_{p1}}{n_1 \cdot V_t} \cdot \exp\left(\frac{(I + I_{s1} + I_{ph}) \cdot R_{p1}}{n_1 \cdot V_t}\right)\right)
$$

$$
+ (I + I_{s1} + I_{ph}) \cdot R_{p1}, \tag{5}
$$

and

$$
V_{d2}(I) = n_2 \cdot V_t \cdot W_0\left(\frac{I_{s2} \cdot R_{p2}}{n_2 \cdot V_t} \cdot \exp\left(\frac{-(I - I_{s2}) \cdot R_{p2}}{n_2 \cdot V_t}\right)\right)
$$

$$
+ (I - I_{s2}) \cdot R_{p2}. \tag{6}
$$

The subscripts 1 and 2 for n and I_s correspond to the upper and lower diodes in Fig. 1b, respectively. These equations could be easily implemented in the spreadsheet software Microsoft Excel as VBA functions, and the device parameters were estimated by fitting the data mentioned in the previous experimental study [12] with the models using Solver add-in program of Microsoft Excel. The fitting was carried out so as to minimize the sum of square of the deviation of voltages at given currents.

2.1 Results and discussion Figure 2a shows the fitting results for the experimental current density–voltage characteristics of p-DTS(FBTTh$_2$)$_2$:C$_{70}$ photocells [12]. The three types of the models, namely the one-diode model and the opposed two-diode model with and without R_s, were used for the fitting. The diode ideality factor was fixed to 1.92, which was obtained by the dark current–voltage characteristics of the photocell [12, 19].

It seems that theoretically-based guideline to choose the ideality factors of the opposed two-diode model has never been established. Traditionally, very different and large values such as $n_1 = 6.5$ and $n_2 = 3.0$ were empirically chosen [8]. At the initial stage of the present study, it has been confirmed that such ideality factors can reproduce the experimental data as shown in Fig. 2b. However, the standard theories of semiconductor diode do not seem to validate such large ideality factors [20, 21]. The opposed two-diode model is reduced to the one-diode model when $I_{s2} = 0$. Therefore, it seems reasonable to estimate the value of n_1 from the dark current–voltage characteristics of the photocell. After some fitting trials, it was found that the reasonably small and single ideality factor estimated from the dark characteristics can reproduce the experimental curve without serious reduction of the fitting accuracy. Similar insensitiveness of the fitting accuracy to the ideality
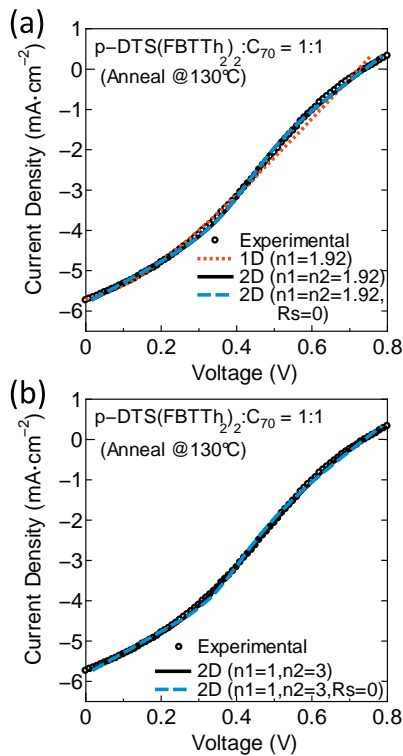
Figure 2 Fitting results for the experimental current density–voltage characteristics of p-DTS(FBTTh$_2$)$_2$:C$_{70}$ photocells with various equivalent-circuit models. 1D and 2D, respectively, refer the one-diode and the opposed two-diode model. (a) and (b) correspond to $n_1 = n_2 = 1.92$ and $n_1 = 1.00$ as well as $n_2 = 3.00$, respectively. The experimental data are identical to those reported in Ref. [12].

Figure 3 Dependence of deviations of fitted voltage from experimental data on the current density; (a) and (b) correspond to $n_1 = n_2 = 1.92$ and $n_1 = 1.00$ as well as $n_2 = 3.00$, respectively.

factor was also observed in the one-diode model [19]. The fitting curve based on the one-diode model obviously deviates from the experimental data, because it cannot reproduce the S-shaped characteristics. On the other hand, the opposed two-diode model seems to give reasonable fitting curves at first glance regardless of the exclusion of R_s.

The deviations of fitted voltages from experimental data are plotted against current density in Fig. 3. Besides large fitting error found in the case of the one-diode model, it is noticed that the exclusion of the series resistance R_s causes substantial increase of fitting error, regardless of the ideality factors chosen. It has been pointed out that the role of R_s can be included in R_{p2} in the preceding studies [8, 18]. However, the present result clearly suggests that the fitting accuracy can be seriously reduced by such approximation, probably because of the reduced flexibility in the circuit model. To the best of the autho's knowledge, the fitting of the S-shaped current–voltage characteristics of photocell with the opposed two-diode model without further simplification to the model has never been reported so far.

The device parameters extracted by the fitting as well as RMS fitting error are summarized in Table 1. The parameters for the one-diode model found in the present
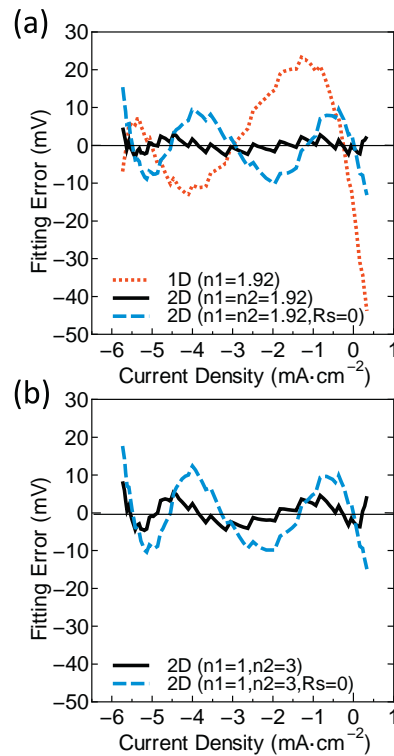
study are not identical to those in the previous study, because the fitting of the present and previous studies was carried out so as to find the best fitted voltages at given currents and the best fitted currents at given voltages, respectively. If the role of R_s can be included in R_{p2} as suggested in the preceding studies, the major effect of the exclusion of R_s must be the increase of R_{p2}. However, what we observed was the reduction of R_{p2}, accompanied by the serious alteration of other device parameters such as the reverse saturation currents of the diodes. This result also suggests that the exclusion of R_s from the opposed two-diode model does not have the straightforward and simple meaning mentioned in the preceding studies.

3 Conclusion In this study, the extraction of the device parameters of an organic photocell which shows S-shaped current–voltage characteristics by fitting with the opposed two-diode model without further simplification to the model was carried out. The easy and straightforward implementation of curve fitting method with commercial spreadsheet software Microsoft Excel employing Lambert *W*-function mentioned in the present study seems to be useful for the experimental researchers of photocells who are not familiar with programming. Besides, the major findings in the present study can be summarized as follows.

1. Although preceding studies empirically chose very different and questionable large values for the ideality

Table 1 Device parameters extracted by the fitting and RMS fitting error.

model	one-diode	two-diode (4 cases)			
n_1	1.92 (fixed)	1.92 (fixed)	1.92 (fixed)	1.00 (fixed)	1.00 (fixed)
n_2	–	1.92 (fixed)	1.92(fixed)	3.00 (fixed)	3.00 (fixed)
J_{S1} (nA cm^{-2})	2.9	1.6	1.3	2.0×10^{-6}	1.7×10^{-6}
J_{s2} (nA cm^{-2})	–	1.6×10^5	6.3×10^4	6.0×10^5	2.0×10^4
J_{ph} (mA cm^{-2})	6.7	8.0	8.2	9.0	8.2
$R_s \cdot A$ (Ω cm^2)	90	45	0 (fixed)	53	0 (fixed)
$R_{p1} \cdot A$ (Ω cm^2)	5.7×10^2	1.9×10^2	1.8×10^2	1.5×10^2	1.6×10^2
$R_{p2} \cdot A$ (Ω cm^2)	–	1.9×10^2	1.3×10^2	8.4×10^2	1.3×10^2
RMS error (mV)	14	1.6	6.6	3.0	7.7

factors of the opposed two-diode model, reasonably small and single value can be used for the ideality factors without the alteration of the fitting accuracy. In other words, the fitting accuracy is rather insensitive to the ideality factors.

2. The series resistance R_s in the opposed two-diode model seriously affects the fitting results, suggesting that the role of it cannot be included in one of the parallel resistances.

Appendix: Equations for calculating Lambert W-function In this study, the Lambert W-function was calculated by using the iteration scheme [15, 22]

$$w_{j+1} = w_j - \frac{w_j \cdot \exp(w_j) - x}{\exp(w_j) \cdot (w_j + 1) - \frac{(w_j+2)\left(w_j \cdot \exp(w_j) - x\right)}{2w_j+2}} \quad (7)$$

with the initial guess obtained by [23]

$$W_0(x) \approx \begin{cases} 0.665 \cdot (1 + 0.0195 \cdot \ln(x+1)) \\ \times \ln(x+1) + 0.04; \ \text{for } 0 \le x \le 500 \\ \ln(x-4) - \left(1 - \frac{1}{\ln(x)}\right) \cdot \ln(\ln(x)); \\ \text{for } x > 500. \end{cases} \quad (8)$$

A Microsoft Excel file containing VBA codes for calculating Eqs. (4)–(6) using Eqs. (7) and (8) is provided as Supporting Information, online at: www.pss-a.com.

Supporting Information
Additional supporting information may be found in the online version of this article at the publisher's website.

References

[1] A. J. Heeger, Adv. Mater. **26**, 10 (2014).
[2] G. Li, R. Zhu, and Y. Yang, Nature Photon. **6**, 153 (2012).
[3] F. C. Krebs, Sol. Energy Mater. Sol. Cells **93**, 394 (2009).
[4] J. P. Charles, M. Abdelkrim, Y. H. Muoy, and P. Mialhe, Sol. Cells **4**, 169 (1981).
[5] M. Chegaar, Z. Ouennoughi, and A. Hoffman, Solid-State Electron. **45**, 293 (2001).
[6] D. Gupta, M. Bag, and K. S. Narayan, Appl. Phys. Lett. **92**, 093301 (2008).
[7] F. A. de Castro, J. Heier, F. Nuesch, and R. Hany, IEEE J. Sel. Top. Quantum Electron. **16**, 1690 (2010).
[8] G. del Pozo, B. Romero, and B. Arredondo, Sol. Energy Mater. Sol. Cells **104**, 81 (2012).
[9] K. Ishibashi, Y. Kimura, and M. Niwano, J. Appl. Phys. **103**, 094507 (2008).
[10] J. Cai, N. Satoh, M. Yanagida, and L. Han, Rev. Sci. Instr. **80**, 115111 (2009).
[11] C. Zhang, J. Zhang, Y. Hao, Z. Lin, and C. Zhu, J. Appl. Phys. **110**, 064504 (2011).
[12] K. Tada, Sol. Energy Mater. Sol. Cells **130**, 331 (2014).
[13] A. Jain and A. Kapoor, Sol. Energy Mater. Sol. Cells **81**, 269 (2004).
[14] A. Oritz-Conde, D. Lugo-Munoz, and F. J. Garcia-Sanchez, IEEE J. Photovolt. **2**, 261 (2012).
[15] R. Corless, G. Gonnet, D. Hare, D. Jeffery, and D. Knuth, Adv. Comput. Math. **5**, 329 (1996).
[16] T. C. Banwell and A. Jayakumar, Electron. Lett. **36**, 291 (2000).
[17] T. C. Banwell, IEEE Trans. Circ. Syst. I **47**, 1621 (2000).
[18] B. Romero, G. del Pozo, and B. Arrendondo, Sol. Enery **86**, 3026 (2012).
[19] K. Tada, Appl. Phys. Express **7**, 051601 (2014).
[20] C.-T. Sah, R. N. Noyce, and W. Shockley, Proc. IRE **45**, 1228 (1957).
[21] W. Shockley and H. J. Queisser, J. Appl. Phys. **32**, 510 (1961).
[22] F. Chapeau-Blondeau and A. Monir, Comput. IEEE Trans Sig. Process. **50**, 2160 (2002).
[23] A. Ringwald and F. Schrempp, Comput. Phys. Commun. **132**, 267 (2000).